Food and Chemical Toxicology 128 (2019) 35–45

Contents lists available at ScienceDirect

Food and Chemical Toxicology

journal homepage: www.elsevier.com/locate/foodchemtox

# The extra virgin olive oil phenolic oleacein is a dual substrate-inhibitor of catechol-O-methyltransferase

Elisabet Cuyàs[a,b], Sara Verdura[a,b], Jesús Lozano-Sánchez[c,d], Ignacio Viciano[e], Laura Llorach-Parés[e], Alfons Nonell-Canals[e], Joaquim Bosch-Barrera[b,f,g], Joan Brunet[f,g,h,i], Antonio Segura-Carretero[c,d], Melchor Sanchez-Martinez[e], José Antonio Encinar[j,*], Javier A. Menendez[a,b,**]

[a] ProCURE (Program Against Cancer Therapeutic Resistance), Metabolism & Cancer Group, Catalan Institute of Oncology, Girona, Spain
[b] Girona Biomedical Research Institute (IDIBGI), Girona, Spain
[c] Department of Analytical Chemistry, Faculty of Sciences, University of Granada, Granada, Spain
[d] Research and Development Functional Food Centre (CIDAF), PTS Granada, Granada, Spain
[e] Mind the Byte, Barcelona, Spain
[f] Medical Oncology, Catalan Institute of Oncology (ICO) Dr. Josep Trueta University Hospital, Girona, Spain
[g] Department of Medical Sciences, Medical School University of Girona, Girona, Spain
[h] Hereditary Cancer Programme, Catalan Institute of Oncology (ICO), Bellvitge Institute for Biomedical Research (IDIBELL) L'Hospitalet del Llobregat, Barcelona, Spain
[i] Hereditary Cancer Programme, Catalan Institute of Oncology (ICO) Girona Biomedical Research Institute (IDIBGI), Girona, Spain
[j] Institute of Research, Development and Innovation in Biotechnology of Elche (IDiBE) and Molecular and Cell Biology Institute (IBMC), Miguel Hernández University (UMH), Elche, Spain

ARTICLE INFO

*Keywords:*
Extra virgin olive oil
Polyphenols
Secoiridoids
Oleacein
COMT
Cancer

ABSTRACT

Catechol-containing polyphenols present in coffee and tea, while serving as excellent substrates for catechol-O-methyltransferase (COMT)-catalyzed O-methylation, can also operate as COMT inhibitors. However, little is known about the relationship between COMT and the characteristic phenolics present in extra virgin olive oil (EVOO). We here selected the EVOO dihydroxy-phenol oleacein for a computational study of COMT-driven methylation using classic molecular docking/molecular dynamics simulations and hybrid quantum mechanical/molecular mechanics, which were supported by *in vitro* activity studies using human COMT. Oleacein could be superimposed onto the catechol-binding site of COMT, maintaining the interactions with the atomic positions involved in methyl transfer from the S-adenosyl-L-methionine cofactor. The transition state structure for the *meta*-methylation in the O5 position of the oleacein benzenediol moiety was predicted to occur preferentially. Enzyme analysis of the conversion ratio of catechol to O-alkylated guaiacol confirmed the inhibitory effect of oleacein on human COMT, which remained unaltered when tested against the protein version encoded by the functional Val$^{158}$Met polymorphism of the *COMT* gene. Our study provides a theoretical determination of how EVOO dihydroxy-phenols can be metabolized *via* COMT. The ability of oleacein to inhibit COMT adds a new dimension to the physiological and therapeutic utility of EVOO secoiridoids.

## 1. Introduction

Human catechol-*O*-methyltransferase (COMT) is a phase II detoxifying enzyme (UniProt code P21964) that catalyzes the transfer of a methyl moiety from the S-adenosyl-L-methionine (SAM) cofactor to one of the hydroxyl groups present in endogenous neurotransmitters (e.g., catecholamines) and hormones (e.g., estradiol), and also xenobiotic substances that incorporate catecholic structures (Bai et al., 2007; Mannisto and Kaakkola, 1999; Zhu and Conney, 1998).

Various catechol-containing coffee and tea polyphenols have been described as excellent substrates for COMT-mediated *O*-methylation (Zhu and Liehr, 1996; Zhu et al., 2000, 2001, 2009). Catechol-

* Corresponding author. Instituto de Investigación, Desarrollo e Innovación en Biotecnología Sanitaria de Elche (IDiBE), Av. de la Universidad, Edif. Torregaitan, Despacho 2.08, E-03202, Elche, Alicante, Spain.
** Corresponding author. Catalan Institute of Oncology (ICO), Girona Biomedical Research Institute (IDIBGI), Edifici M2, Parc Hospitalari Martí i Julià, E-17190, Salt, Girona, Spain.
*E-mail addresses:* jant.encinar@umh.es (J.A. Encinar), jmenendez@iconcologia.net, jmenendez@idibgi.org (J.A. Menendez).

https://doi.org/10.1016/j.fct.2019.03.049
Received 26 February 2019; Received in revised form 25 March 2019; Accepted 26 March 2019
Available online 29 March 2019
0278-6915/ 

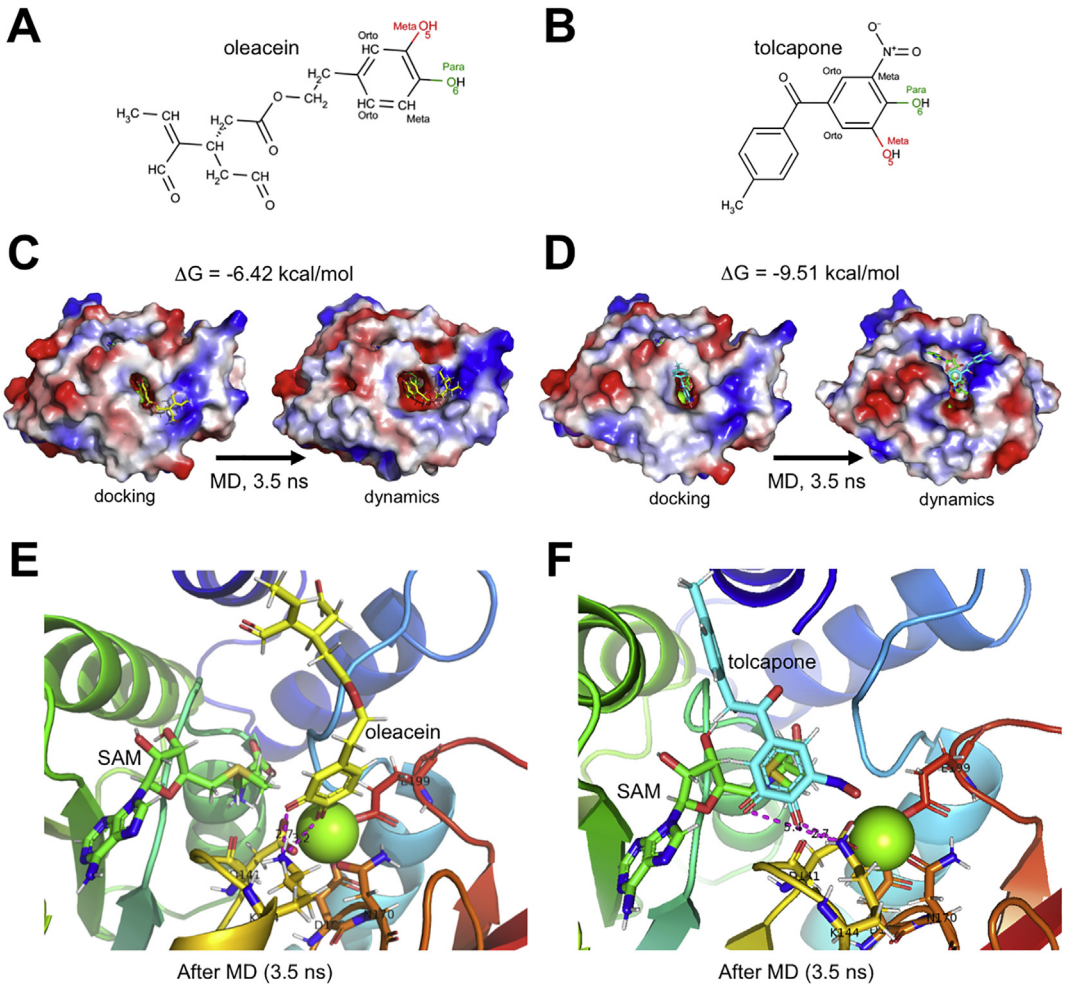


**Fig. 1.** Interactions of oleacein and tolcapone with the catalytic binding site of the native COMT enzyme. Molecular structure of oleacein (panel **A**) and tolcapone (panel **B**). The position of the hydroxyl groups in *meta*-O5 and *para*-O6 of the aromatic ring is indicated. Left figure in panels **C** and **D** shows the best pose of oleacein and tolcapone coupled to the catalytic binding site of native COMT (3BWM) represented as an electrostatic surface potential. The right figure on panels **C** and **D** shows the COMT-oleacein and -tolcapone enzyme complexes after 3.5 ns of molecular dynamics simulation. The protein has been represented as an electrostatic surface potential and the water molecules and the $Na^+$ and $Cl^-$ ions have been eliminated to facilitate visualization. Above the left figure of panels **C** and **D** is the Gibbs free energy variation calculated with AutoDock/vina v1.1.2 (Trott and Olson, 2010). Panels **E** and **F** show details of the interactions between oleacein and tolcapone, respectively, with native COMT after 3.5 ns of molecular dynamics simulation. The backbone is represented in the form of ribbons and rainbow color. Both the oleacein and tolcapone structures are shown in stick format and the $Mg^{2+}$ atom as a light green sphere. S-adenosyl-L-methionine (SAM) is represented as sticks. The amino acids involved in the formation of coordination bonds with $Mg^{2+}$ are shown as sticks and numbered. The figure was built using PyMol 2.0 software. (For interpretation of the references to color in this figure legend, the reader is referred to the Web version of this article.)

containing natural polyphenols can also behave as COMT inhibitors, impeding the *O*-methylation of a variety of catechol substrates. Such a dual mechanism has been explained in terms of either direct competitive inhibition of the COMT catalytic center by the catecholic polyphenols themselves, or by non-competitive inhibition due to the elevated levels of demethylated SAM (S-adenosyl-L-homocysteine [SAH]), a very potent feedback inhibitor of various SAM-dependent methyltransferases including COMT itself and DNA methyltransferases (DNMTs), which is generated during the rapid formation of COMT-formed *O*-methylated derivatives (Bai et al., 2007; Nagai et al., 2004; Zhu, 2002; Zhu and Liehr, 1994; Zhu et al., 2008, 2010). Indeed, given that COMT and DNMT belong to the same family of SAM-dependent methyltransferases with common core catalytic structures, catechol-containing dietary polyphenols may operate as cumulative factors that affect the rate of DNA methylation not only *via* SAH-related indirect mechanisms, but also *via* direct inhibitory occupancy of DNMT catalytic centers (Fang et al., 2003, 2007; Lee et al., 2005).

Extra virgin olive oil (EVOO) is the oil extracted from the fruits of olive trees solely by mechanical means and consumed without further refinement. There is increasing evidence that EVOO phenols exert potent biological activities that could account for the health-promoting effects of the "Mediterranean Diet" (Angeloni et al., 2017; Colomer et al., 2008; Crespo et al., 2018; Fuccelli et al., 2018; Lopez-Miranda et al., 2010; Nikou et al., 2019; Rigacci, 2015; Tomé-Carneiro et al., 2017). Quantitatively, the class of phenol-conjugated compounds termed oleosidic secoiridoids or oleosides is the most represented in the phenolic fraction of EVOO (Bendini et al., 2007; Servili et al., 2009). The main EVOO secoiridoids are oleuropein and ligstroside, the aglycones of which are esters of elenolic acid with hydroxytyrosol or tyrosol, respectively. Other secoiridoids are oleacein and oleocanthal, the dialdehydic forms of decarboxymethyl elenolic acid bound to hydroxytyrosol or tyrosol, respectively (Casamenti and Stefani, 2017; Corominas-Faja et al., 2014; Menendez et al., 2013; Vazquez-Martin et al., 2012). Interestingly, the main biological metabolite of hydroxytyrosol (Serreli et al., 2019), which is present as a simple phenolic compound and mainly as conjugated forms in secoiridoids, is 3-O-methyl-hydroxytyrosol, an *O*-methylated product generated by COMT (De la Torre et al., 2017; Miro-Casas et al., 2003). However, despite the

considerable effort expended on characterizing the dual COMT substrate-inhibitor behavior of major polyphenolic components present in coffee and tea, almost no studies have directly explored the relationship between COMT and the dietary phenolics existing in EVOO.

Previous studies in our laboratory revealed how the absorption process and metabolic conversion of the multiple compounds present in the EVOO phenolic fraction could take place at the cellular level (Garcia-Villalba et al., 2012). Members of the secoiridoids family of EVOO phenolics were the most rapidly absorbed and extensively metabolized, mainly as methyl-conjugates. Remarkably, methylated derivatives were exclusively observed not only for catechol-containing luteolin but also for single hydroxytyrosol and hydroxytyrosol-containing oleuropein aglycone and oleacein. Conversely, no methyl-conjugates could be found for secoiridoids derived from tyrosol (i.e., ligstroside aglycone and D-ligstroside aglycone). Our findings using human breast cancer epithelial cells were in line with previous studies using Caco-2 cells as a model of the human intestinal epithelium and HepG2 cells as a model of the human liver, in which methylated derivatives of hydroxytyrosol-containing phenolics were the major metabolites detected (Goya et al., 2007; Manna et al., 2000; Soler et al., 2010). Because COMT-driven methylation requires the presence of an ortho (O)-diphenolic structure, overall these findings strongly suggested that EVOO dihydroxy-phenols could be preferentially metabolized *via* COMT-catalyzed *O*-methylation.

Here, we selected the EVOO-derived dihydroxy-phenol oleacein to carry out the first virtual computational study of COMT-driven methylation of EVOO biophenols using classic molecular docking and molecular dynamics (MD) simulations, as well as hybrid quantum mechanical/molecular mechanics, which was followed by *in vitro* activity studies using human COMT.

## 2. Results

### 2.1. Molecular docking simulation of the oleacein-COMT complex: a comparative study with the COMT inhibitor tolcapone

We carried out a classic molecular docking approach using oleacein (Fig. 1A), the second-generation COMT inhibitor tolcapone (Fig. 1B), and the complete structure of the COMT enzyme (Protein Data Bank [PDB] code 3BWM). The catalytic binding site of COMT for a catechol ligand consists of a pocket in which the hydroxyl group must be placed in the *para* position mono-coordinated to $Mg^{2+}$. The cofactor SAM is in a nearby position to serve as the methyl donor (Tsao et al., 2011).

We initially sought to evaluate whether the interaction of oleacein and tolcapone with COMT preferentially took place at the catalytic binding site. Rigid docking simulations of tolcapone produced up to three clusters of docking poses that were located in the vicinity of the COMT catalytic site (Fig. 1C and D). Tolcapone binding energies reached −9.51 kcal/mol in the #1 ranked cluster. By contrast, rigid docking simulations of oleacein indicated that the top-two ranked clusters were located away from the catalytic binding site. The best pose of oleacein that coupled to the catalytic site of COMT (#3 ranked cluster) showed a binding energy of −6.42 kcal/mol. The tolcapone molecule exhibiting the best binding energy in cluster #1 and the oleacein molecule in cluster #3 were subsequently chosen for MD simulations.

### 2.2. Molecular dynamics simulation of the oleacein-COMT complex: a comparative study with the COMT inhibitor tolcapone

While molecular docking simulations can be applied to explore and predict the binding modes of a substrate to an enzyme (by extension, to any other biomolecule), MD can provide additional information about different intra- and inter-molecular movements over time (Land and Humble, 2018; Maximova et al., 2016). Thus, to add protein flexibility to the analysis of the oleacein-COMT and tolcapone-COMT complexes, we carried out short MD simulations over the course of 100 ns.

Two notable differences were observed when comparing the MD-predicted interactions of oleacein and tolcapone with the surface of the catalytic binding site of COMT (Fig. 1E and F). In the case of tolcapone, a rearrangement of the side chains of the amino acids of the catalytic site takes place during the first nanosecond of MD simulation. In the case of oleacein, however, those changes in the surface of the catalytic binding site cannot be observed in the first 3.5 ns of MD simulation. Such a rearrangement of the side chains presents a cavity that allows visualizing the SAM cofactor. Moreover, while the oleacein hydroxyl group in position *para*-O6 is positioned in a plane superior to $Mg^{2+}$ at a suitable distance to form a coordination bond between them before the first 3.5 ns of MD simulation, we noted that the equivalent hydroxyl group in tolcapone moves away from the coordination distance with $Mg^{2+}$. The sphere of coordination with $Mg^{2+}$ is maintained by the residues Asn170, Glu199 and Asp141 in the same coordination plane; and by the residue Asp169 in a lower plane.

We assumed that the hydroxyl group of oleacein was deprotonated in a previous step, as occurs for other COMT substrates including catechol. The amino group of Lys144 is believed to be responsible for such deprotonation, which can occur at physiological pH (Brandt et al., 2015; Kiss and Soares-da-Silva, 2014; Sparta and Alexandrova, 2012; Tsao et al., 2011). Indeed, the distance between the deprotonated oxygen *para*-O6 and *meta*-O5 of oleacein and the amino group was 3.2 Å and 2.7 Å, respectively (Fig. 1E), making deprotonation by the lysine residue plausible. In such a scenario, the *para*-O6 of the oleacein molecule would be located at a suitable distance to formalize a coordination bond with $Mg^{2+}$, in a plane superior to that defined by the triad Asn170, Glu199 and Asp141. The *meta*-O5 would also be at a suitable distance from the SAM cofactor to receive its methyl group in the course of the reaction catalyzed by COMT. By contrast, neither of the two hydroxyl groups of the aromatic ring of the tolcapone molecule appeared to perform chelation with the $Mg^{2+}$ ion (Fig. 1F). This situation likely explains why the position of tolcapone becomes drastically altered throughout the MD simulation with respect to the initial event of rigid molecular docking. These observations overall predicted that, while oleacein could behave as a COMT substrate whose catalysis would generate *meta*-O5 methyl-oleacein as a product, such a substrate nature cannot be observed in the case of tolcapone. Therefore, it appears that the behavior of a given molecule as a COMT substrate (e.g., oleacein) necessarily requires the establishment of a sphere of coordination between the *para*-O6 hydroxyl group and $Mg^{2+}$, whereas such an interaction is not required to show an inhibitory behavior (e.g., tolcapone). Accordingly, experimental data have shown that only 2.1% of metabolized tolcapone can be found as circulating *meta*-O5 methyl tolcapone in human plasma (Jorga et al., 1999).

### 2.3. Virtual computational simulation of COMT-catalyzed oleacein methylation

Our simulation system took advantage of a previous study revealing the coordinates of the transition state (TS) structure found for the SAM-dependent catechol methylation reaction occurring in the active site of COMT (Kulik et al., 2016). The stationary structures obtained (i.e., reactants [R], transition states [TS], and products [P]) following both oleacein and tolcapone methylations in meta-O5 positions are shown in Fig. 2. The COMT protein backbone root mean square deviation (RMSD) plots of the ligands heavy atoms **R**, SAM *versus* oleacein or tolcapone (Fig. 2A and D), **TS**, SAH and methyl *versus* oleacein or tolcapone (Fig. 2B and E), and **P**, SAH *versus meta*-O5 methyl oleacein (Fig. 2C) or *para*-O6 methyl oleacein or *meta*-O5 methyl tolcapone (Fig. 2F) or *para*-O6 methyl tolcapone, measured after superimposing COMT on its reference structure during the 100 ns period of the MD simulation, are shown in Fig. 3. These MD simulations of the ligand-protein complexes included also the protein version containing the functional $Val^{158}Met$ (V108M) polymorphism of the COMT gene, which

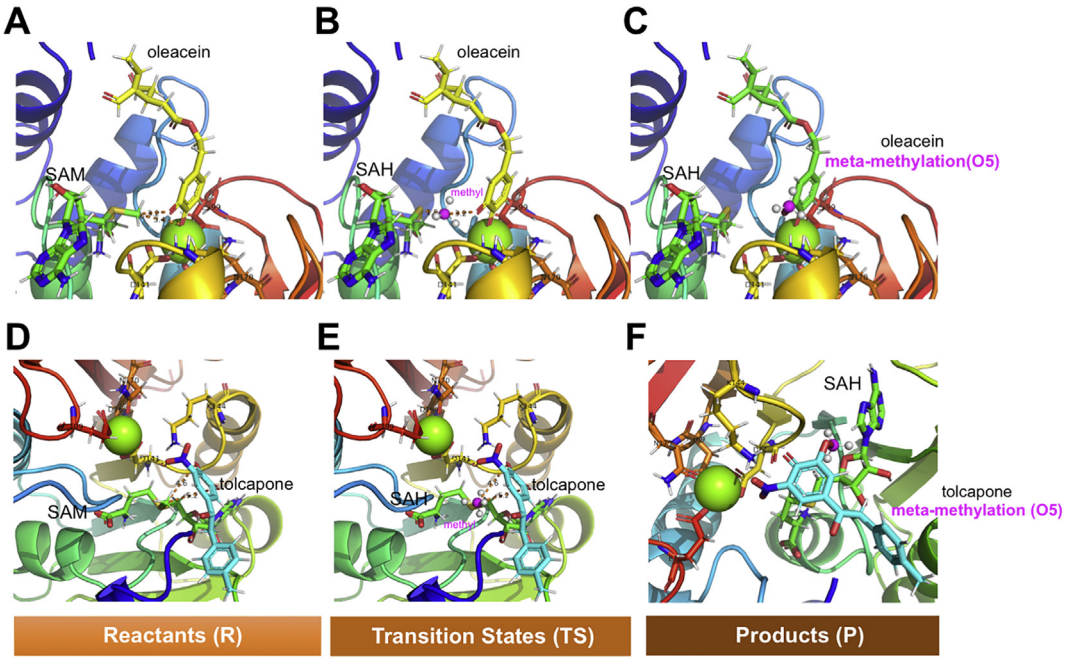


**Fig. 2.** Representation of the stationary structures corresponding to reactants (R, panels **A** and **D**), transition states (TS, panels **B** and **E**), and products (P, panels **C** and **F**) by methylation of a single oleacein or tolcapone hydroxyl to form the *meta*-O5 methylated product. The snapshot corresponds to the 3.5 ns time of the molecular dynamics simulation. The amino acids involved in the formation of coordination bonds with $Mg^{2+}$ are shown as sticks and numbered, and the $Mg^{2+}$ atom as a light green sphere. S-adenosyl-L-methionine (SAM) and S-adenosyl-L-homocysteine (SAH) are represented as sticks. The water molecules and the $Na^{+}$ and $Cl^{-}$ ions have been eliminated to facilitate visualization. The figure was built using PyMol 2.0 software. (For interpretation of the references to color in this figure legend, the reader is referred to the Web version of this article.)

presents lower enzymatic activity than the parental form in addition to lower expression levels *in vivo* (Rutherford et al., 2008). Although M108 (PDB code 3BWY) is found at about 16 Å from SAM, the interactions of its lateral chain with the residues Ala22 and Arg78 presume a displacement of the protein backbone of 0.7 Å that propagates through SAM to the catalytic binding site (Rutherford et al., 2008).

Careful analysis of the ligand movements in the binding pockets of COMT and COMT V108M indicated that, in the case of oleacein, the position of R, TS and P (*meta*-O5- or *para*-O6-methyl oleacein) remains constant from 10 ns with respect to the starting structure (i.e., that resulting from the molecular docking of oleacein to the holoenzyme) at time 0 ns, not only for the parental form of COMT but also for the V108M form (Fig. 4A,C). A completely different picture emerged, however, in the case of tolcapone (Fig. 4B,D); in the parental form of COMT, only tolcapone in the TS remains constant in its position at the catalytic binding site, whereas both R and P (*meta*-O5- or *para*-O6-methyl tolcapone) shift (60 ns from the beginning of the MD simulation) to an average of 30 Å with respect to the starting structure (resulting from the molecular docking of tolcapone to the holoenzyme) at time 0 ns. In the case of V108M COMT, only tolcapone in R undergoes a large movement (40 ns from the beginning of the MD simulation) of about 35 Å; yet, *meta*-O5 methyl tolcapone in R shows an up movement of about 10 Å with respect to the site initially occupied at the beginning of the MD simulation. These data suggest that, although both R (i.e., tolcapone) and P (*meta*-O5-methyl or *para*-O6-methyl tolcapone) could behave as noncompetitive COMT inhibitors, the P forms of tolcapone are predicted to be rarely generated. Most of the changes in the secondary structural motifs (i.e., helix, sheet, coil, turn, radius of gyration, and hydrogen bonds) of parental and V108M COMT were small, with the exception of some structures including tolcapone (Supplementary Figs. S1–S7).

To further verify the stability of the protein-ligand complexes, we carried out an evaluation of the Molecular Mechanics/Poisson-Boltzmann Surface Area (MM/PBSA) parameter (Wang et al., 2016), which estimates the free energy of the binding of small ligands to biological macromolecules, uses MD simulations of the receptor-ligand complex, and is known to show good correlations with the values obtained experimentally despite excluding the conformational entropy or the number and free energy of water molecules in the binding site (Genheden and Ryde, 2015; Wang et al., 2016) (Fig. 5). The values of free energy calculated for the union of oleacein to parental COMT and V108M COMT show negative values for R, TS and P *meta*-O5 methylation and *para*-O6 methylation and, consequently, we cannot predict a stable and strong binding to the enzyme (Fig. 5A,C). The average binding energy (calculated as the average of the last 10 ns or during the 100 ns of total duration of the MD) shows similar (negative) values for the parental COMT- or V108M-oleacein (and products) complexes; the product *para*-O6-methyl oleacein shows a very unfavorable binding energy (above −315 kcal/mol) for both forms of COMT; the product *meta*-O5-methyl oleacein shows a more favorable binding energy for the parental form of COMT (above −180 kcal/mol) than for V108M COMT (above −190 kcal/mol). The binding energy of R oleacein is better for the V108M form (above −165 kcal/mol) than for the parental form of COMT (about −190 kcal/mol) and, therefore, a lower enzymatic activity of the V108M form of COMT could be predicted; the average binding energy shows similar (positive) values for the parental COMT- or V108M-tolcapone (and products) complexes, therefore predicting an inhibitory role (but not a substrate) of tolcapone for both COMT forms (Fig. 5B,D). The latter notion is supported further by the fact that the methylation products of tolcapone (*meta*-O5-methyl tolcapone and *para*-O6-methyl tolcapone) exhibit not only an early displacement of the catalytic binding site but also higher binding energies than the reactant.

### 2.4. A Quantum Mechanics/Molecular Mechanics (QM/MM) approach to confirm the COMT-driven methylation of oleacein

We sought to theoretically confirm the aforementioned putative methylation mechanism of the EVOO phenolic oleacein by performing Quantum Mechanics/Molecular Mechanics (QM/MM) simulations. This

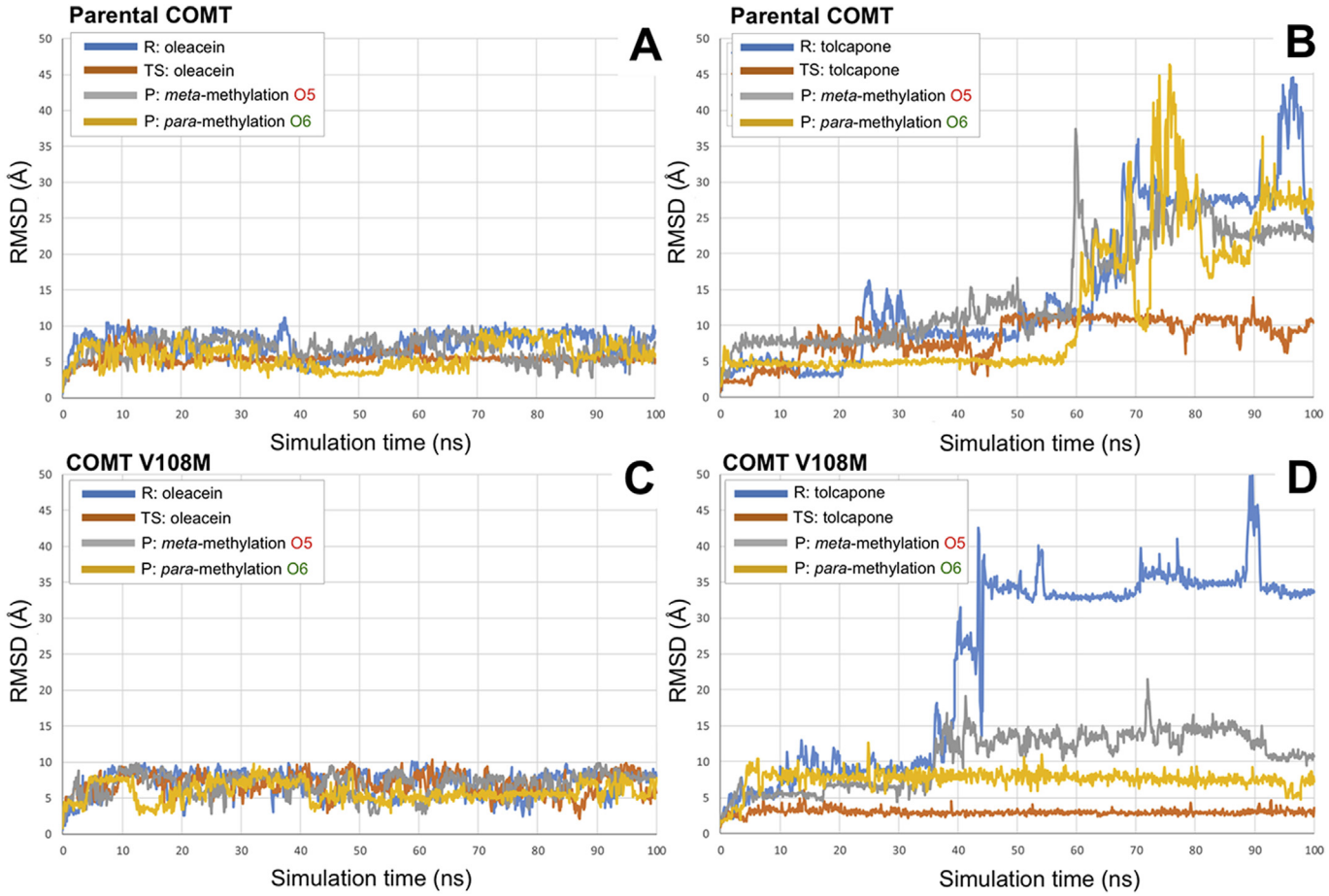


**Fig. 3.** Root mean square deviation of the ligand heavy atoms over simulation time, measured after superposing the protein on its reference structure. In the context of the molecular dynamic simulations presented here, it is considered as a ligand to oleacein or tolcapone in the states of reactants, transition state and Products (*meta*-O5 methylated and *para*-O6 methylated). Panels **A** and **B** show the trajectories of the ligands forming complexes with COMT, whereas panels **C** and **D** show the trajectories of the different ligands forming complexes with the V108M COMT. Shown within each panel is the legend that indicates the correspondence with each ligand.

is a hybrid computation approach widely used in studies of enzymatic catalysis in which the region of primary interest is treated quantum mechanically, while the surrounding portion of the enzyme is described with an empirical molecular mechanics model (Kamerlin et al., 2009; Viciano et al., 2015; Kulik et al., 2016; Roston and Cui, 2016).

We performed QM/MM calculations to theoretically describe the reaction in which a methyl group is transferred in a $S_N2$ reaction from SAM to the deprotonated alcohol of oleacein. Because both hydroxyl groups of the benzenediol moiety of oleacein were predicted to be susceptible to deprotonation and, therefore, they might act as attacking nucleophiles, we studied the transfer reaction for both *meta*-methylation in the position O5 and *para*-methylation in the position O6. To evaluate such chemical reactivity, the region of primary interest was treated quantum mechanically and included the SAM cofactor, the oleacein molecule, and the $Mg^{2+}$ ion. These atoms were described by the density functional theory (B3LYP) methodology using the 6–31(d,p) basis set. The surrounding portion of the enzyme was described by means of empirical MM using the all-atoms optimized potentials for liquid simulations (OPLS-AA) force field for the protein and the TIP3P potential for the water molecules. Once TS were localized, they were characterized by Hessian inspection and minimum energy paths were traced down to their corresponding minima, thereby ensuring that the structures actually connected reactants and intermediates. When comparing the energetic barriers following oleacein methylation in both *meta*- and *para*-positions, we noticed that the *para*-methylation barrier would be actually about twice as high as that for the *meta*-methylation reaction of oleacein (Supplementary Fig. S8). Thus, whereas the potential activation energy for the *meta*-methylation reaction of oleacein was as low as 14 kcal/mol, the corresponding activation energy for the *para*-methylation reaction was calculated as 27 kcal/mol. The first reaction was predicted to occur through an exothermic process while the latter appeared to take place through an endothermic one.

### 2.5. Effects on oleacein on COMT-catalyzed catechol methylation

We finally investigated the inhibitory effect of oleacein on the *O*-methylation of catechol catalyzed by the soluble form of human COMT (s-COMT) using a radiometric assay. The method is based on the conversion of catechol to $^3$H-guiacol by COMT in the presence of $Mg^{2+}$ and methyl $^3$H-labeled SAM (Zurcher and Da Prada, 1982). When graded concentrations (from 0.2 to 100 μmol/L) of oleacein were added to the incubation mixture, the rate of *O*-methylation of catechol by s-COMT was inhibited in a concentration-dependent manner (Fig. 6, *left panel*). The average 50% inhibitory concentration ($IC_{50}$) value of oleacein for inhibiting the *O*-methylation of catechol by s-COMT was 3.08 ± 0.3 μmol/L.

We explored also whether the inhibitory effects of oleacein on s-COMT became altered when tested against the functional version V108M s-COMT. Similar to that observed with the parental s-COMT, when different concentrations of oleacein were added to the incubation mixture the rate of catechol *O*-methylation by V108M s-COMT was also inhibited in a concentration-dependent manner (Fig. 6, *right panel*); the

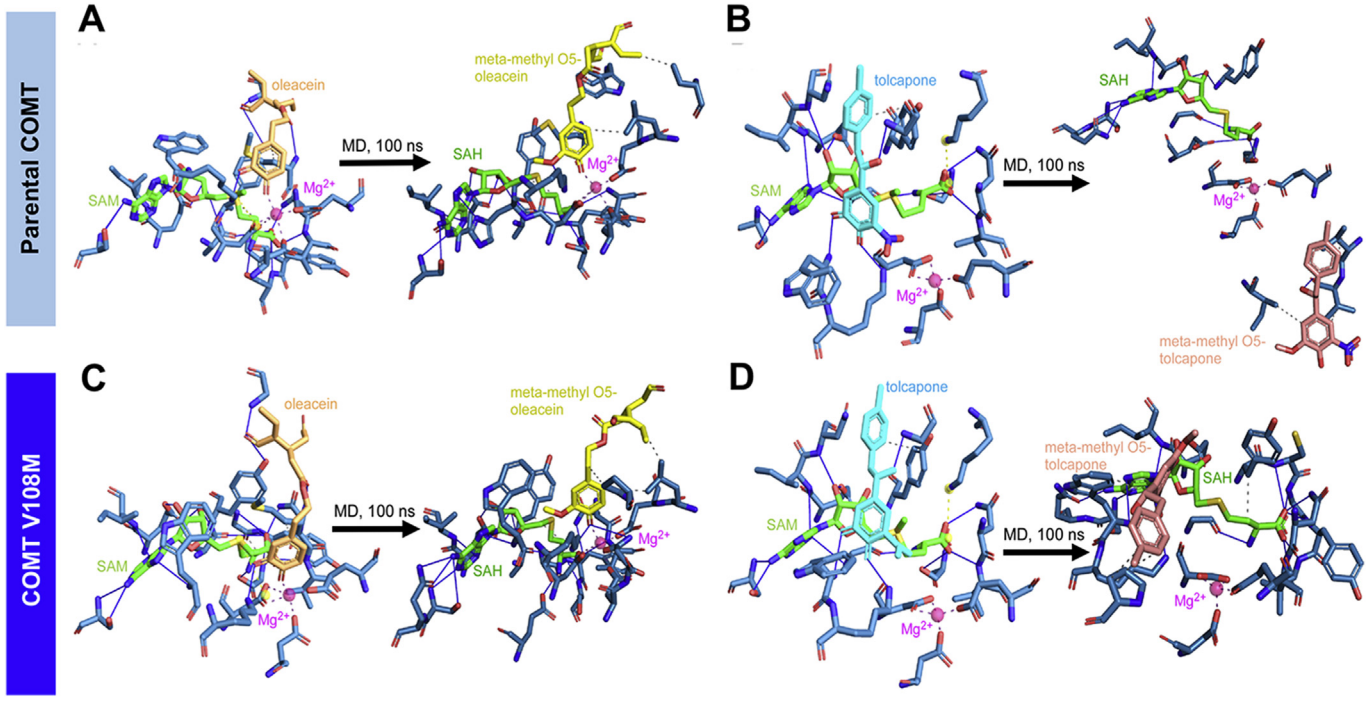


**Fig. 4.** Detail of the interactions of oleacein (left figure in panels **A** and **C**), *meta*-O5 methylated oleacein (right figure in panels **A** and **C**), tolcapone (left figure in panels **B** and **D**), and *meta*-O5 methylated tolcapone (right figure in panels **B** and **D**) compounds complexed to COMT (**A**, **B**) or V108M COMT (**C**, **D**), indicating the amino acids involved and the type of interaction (hydrogen bonds, hydrophobic interactions, salt bridges, π-stacking, etc). The interactions were detected with the FLIP algorithm (Salentin et al., 2015). S-adenosyl-L-methionine (SAM) and S-adenosyl-L-homocysteine (SAH) are represented as sticks and the $Mg^{2+}$ atom as a pink sphere. The figure on the left of each panel corresponds to a snapshot taken at 3.5 ns of the molecular dynamics simulation, while the figure on the right results from the acquisition of a snapshot at 100 ns of the simulation. Water molecules and the $Na^+$ and $Cl^-$ ions have been eliminated to facilitate visualization. The figure was built using PyMol 2.0 software. (For interpretation of the references to color in this figure legend, the reader is referred to the Web version of this article.)

average $IC_{50}$ value of oleacein for inhibiting the O-methylation of catechol by V108M s-COMT was 2.9 ± 0.2 μmol/L, a similar potency to that observed with parental s-COMT.

## 3. Discussion

Our bio-computational approach provides the first theoretical evaluation and experimental confirmation that EVOO dihydroxy-phenols such as the secoiridoid oleacein can operate as dual substrate-inhibitors of COMT.

From our computational studies, we could infer that a deprotonated hydroxyl O5 group of the oleacein molecule is methylated by the SAM cofactor in the active site of COMT. Oleacein is predicted to liberate its *para*-O6 hydroxyl group to form a co-ordinate bond with $Mg^{2+}$, thereby enabling a free *meta*-O5 hydroxyl group to receive a methyl group from SAM to generate SAH and *meta*-O5 methyl oleacein as final products. The transition state structure for the meta-methylation O5 reaction was predicted by QM/MM to occur preferentially over the production of the para-methylation, with methylation energies (14 kcal/mol) even lower than those theoretically (16–22 kcal/mol) and experimentally (18.4 kcal/mol) determined for the catechol molecule (Roca et al., 2003; Sparta and Alexandrova, 2012; Kulik et al., 2016; Jindal and Warshel, 2016). Given that earlier studies have shown that methylated conjugates were the major derivatives detected following oleacein metabolization by cultured cancer cells, it is reasonable to suggest that a critical *in vivo* metabolic step of EVOO dihydroxy-phenols is COMT-catalyzed *O*-methylation. 3-*O*-methyl-hydroxytyrosol, the COMT-derived biological metabolite of the single dihydroxy-phenol hydroxytyrosol, has been shown to exert a protective effect on cardiovascular disease and total mortality (De la Torre et al., 2017). Therefore, it remains of crucial importance to definitively determine whether methylated derivatives of EVOO complex dihydroxy-phenols such as the secoiridoid oleacein are differentially bioactive when compared with their parental compounds, as occurs with *bona fide* catechol-containing polyphenols such as epigallocatechin gallate (Landis-Piwowar et al., 2010; Wang et al., 2012).

From our experimental studies we could confirm that, similar to well-known catechol-containing dietary polyphenols, EVOO secoiridoids such as oleacein can behave as COMT inhibitors capable of suppressing the *O*-methylation of a variety of catechol substrates. The inhibitory potency of oleacein to human COMT-mediated catechol O-methylation remained unaltered when the native COMT protein was substituted by the $Val^{158}$Met genetic variant. The V109M substitution reduces the activity of COMT to one-quarter of the parental *Val* allele (Lachman et al., 1996; McLeod et al., 1998), which has been associated with significant differences in brain function and behavior as well as cancer susceptibility (Antypa et al., 2013; Chen et al., 2016; He et al., 2012; Huang et al., 2016; Klebe et al., 2013; Sak, 2017; Witte and Floel, 2012). Several meta-analyses have suggested that while the COMT $Val^{158}$Met polymorphism might not be a risk factor for overall cancer risk, it may, nevertheless, be involved in cancer development, at least in some ethnic groups or specific cancer types (Zhou et al., 2015). Since low COMT activity and consumption of certain dietary polyphenols have been linked to a decreased risk in breast cancer via a decrease of potentially carcinogenic, circulating estrogens (Wu et al., 2003a; b, 2005), it would be relevant to explore whether the consumption of oleacein-rich EVOO may be more cancer protective in individual carrying the low activity COMT polymorphism (i.e., whether a seeming predictor of oleacein potency *in vivo* may inversely correlate with individual COMT activity status). In a clinical setting, COMT status might therefore be used to determine which individuals would benefit from EVOO consumption/oleacein treatment as a dietary strategy to reduce the onset and recurrence of certain cancers, including breast cancer. Nonetheless, it might also occur that EVOO polyphenol chemicals

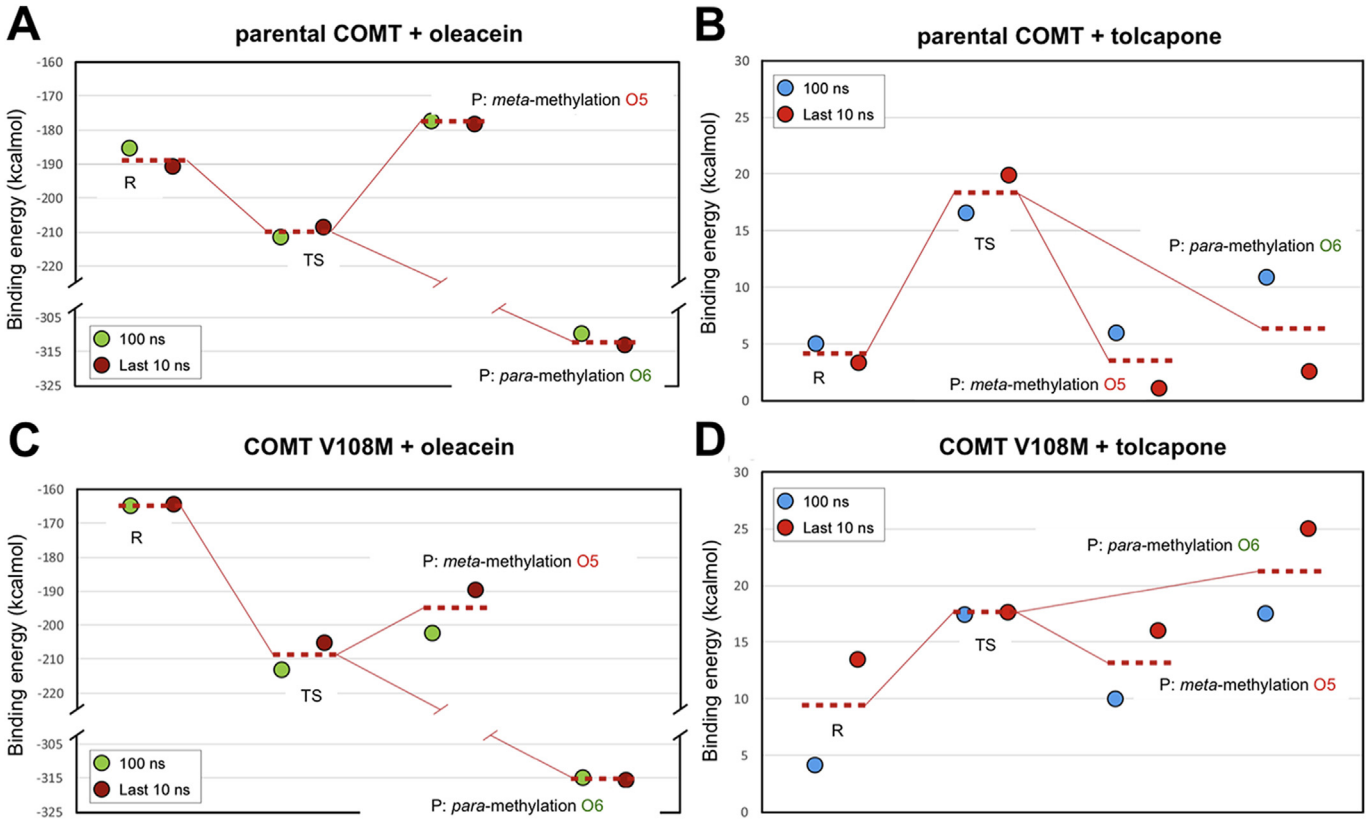


**Fig. 5.** Molecular Mechanics/Poisson-Boltzmann Surface Area free energy analysis of COMT (panels **A** and **B**) and V108M COMT (panels **C** and **D**) forming complexes with reactants, transition states and products of oleacein (**A** and **C**) and tolcapone (**B** and **D**) using YASARA dynamics v18.12.27 software. In each case, the best-docked complex as the initial conformation for the simulation, followed by 1000 snapshots obtained from the molecular dynamics trajectory were employed to calculate the values of free energy binding of the native and polymorphic enzymes. Additionally, the average calculated value of the last 100 snapshots is displayed. YASARA-calculated binding energy presents positive values when the union is stable and strong, whereas negative values indicate no binding (Winkler et al., 2019). The legend included within each panel indicates whether the actual value computes the last 10 ns or the entire simulation time (100 ns).

would require their complex, natural combination forms to exhibit superior chemopreventive or anti-cancer activities as compared with their single components if they depend on interactions with other EVOO phenolic components for efficacy (Bode and Dong, 2009; Sak, 2017; Shimizu et al., 2005; Skates et al., 2018; Suganuma et al., 1999; Wang et al., 2012). Thus, if the bioavailability of a given EVOO phenolic would be increased by suppressing the formation of COMT-derived *O*-methylated metabolites by other phenolic components of the mixture, such synergistic action between phenolic molecules containing catechol-like moieties might be physiologically relevant to understand not only the cancer-preventive actions of EVOO, but also in reducing the risk of other chronic diseases when combined with other phenolic-containing products in the Mediterranean diet (e.g., cardiovascular diseases and moderate consumption of red wine; De la Torre et al., 2017).

Our current findings provide a new scenario in which it would be of interest to evaluate the nature of the anti-tumoral cytotoxic interactions between EVOO dihydroxy-phenols and nitrocatechols such as tolcapone and entacapone, two clinically approved COMT inhibitors in the management of Parkinson's disease (Forester and Lambert, 2014; Kiss and Soares-da-Silva, 2014; Wang et al., 2014). Moreover, the fact that EVOO di-hydroxyphenols such as oleacein can serve as naturally-occurring COMT inhibitors might be exploited for the development of combinatorial strategies aimed at preventing neurodegeneration in some pathological settings such as Alzheimer's and Parkinson's diseases, for example by improving L-DOPA bioavailability *via* suppressing

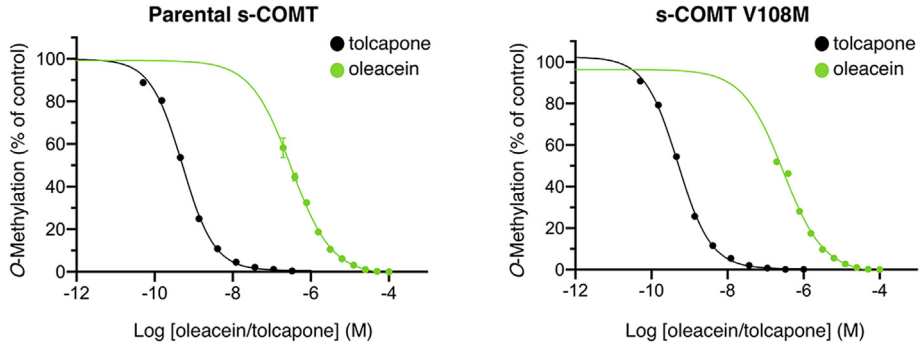


**Fig. 6.** Inhibition of s-COMT- (*left*) and V108M s-COMT- (*right*) mediated O-methylation of catechol by increasing concentrations of oleacein and tolcapone. Each point is the mean of duplicate determinations.

COMT-driven conversion of L-DOPA to 3-O-methyldopa (Kang et al., 2010; Perkovic et al., 2018; Serretti and Olgiati, 2012), or for improving cognitive efficiency in aging (Sambataro et al., 2012). Combinations of natural and synthetic COMT-targeting agents might be more effective (and have fewer side-effects) for preventing or treating aging-related chronic diseases because they would likely require lower doses of the molecular-targeted agents. In this regard, the *in vitro* potency of oleacein in inhibiting COMT-catalyzed catechol methylation (in the low micromolar range) was notably weaker than the second-generation COMT inhibitor tolcapone (which occurred in the low nanomolar range, i.e., $IC_{50}$ = 5.2 and 4.9 nmol/L against s-COMT and V108M s-COMT, respectively). Perhaps more importantly, considering the role of the common COMT rs4680 ($Val^{158}Met$) genotype in determining the cancer-preventive (or lack of) nature of key micronutrients such as vitamin E/α-tocopherol (Hall et al., 2019), it should be noted that oleacein and tolcapone were predicted to operate as COMT substrates/inhibitors *via* highly dissimilar mechanisms, especially regarding their mechanisms of action against the V108M COMT variant. Specifically, the catalytic activity of V108M COMT is not expected to be significantly altered when there is no significant displacement of the substrate/product from the catalytic site, as is the case of oleacein. However, the weakened activity of COMT upon a non-synonymous valine-to-methionine substitution might become relevant when the substrate/product should be evicted from the active site, as is the case of tolcapone.

Because the methyl group with which COMT carries out targeted modification of catechol compounds is provided by the cofactor SAM, the COMT-mediated rapid methylation of large amounts of dietary catechols could be expected not only to reduce the intracellular pools of SAM, but also to generate significant amounts of demethylated SAH. SAH is a very potent non-competitive inhibitor of various SAM-dependent methylation reactions including those catalyzed by COMT and also by DNMTs, and very low concentrations of intranuclear SAH might suffice to cause a meaningful inhibition of enzymatic DNA methylation (Huang et al., 2019; Lee and Zhu, 2006). Our current findings provide a theoretical mechanistic basis for the notion that EVOO dihydroxy-phenols can function as important, indirect modulators of the cellular DNA methylation process through increased formation of SAH during COMT-mediated *O*-methylation. Moreover, because both COMT and DNMTs belong to the same superfamily of SAM-dependent methyltransferases and share a common core structure at the catalytic site (Cheng, 1995; Fang et al., 2003), EVOO dihydroxy-phenols may act as direct inhibitors of DNMTs. Accordingly, we have recently provided computational evidence predicting the ability of oleacein to bind the DNA-binding catalytic pockets of DNMTs, and experimental confirmation that oleacein can function as a direct inhibitor of the SAM-dependent methylation activity of several DNMTs (Corominas-Faja et al., 2018). Hence, EVOO secoiridoids might certainly produce cumulative effects on the rate of DNA methylation through non-competitive inhibition of DNMTs *via* the formation of SAH during their metabolic methylation by COMT, and independently of their own methylation through a direct inhibition of DNMTs.

## 4. Conclusions

The findings of our present study provide new insights into the mechanisms through which EVOO phenolics interact with and alter the functioning of the SAM/SAH-related methylation machinery. While it might be argued that the average daily intake of EVOO dihydroxy-phenols may not represent an overwhelming burden for the SAM-dependent COMT- and DNMT-mediated methylation system, it should be noted that such effects may be notably more significant if a normal diet is substituted by one with limited amounts of methyl donors (e.g. methionine restriction) or if such dual substrate-inhibitors of COMT activity are given as part of mixtures containing COMT- or DNMT-targeted inhibitors.

## 5. Materials and methods

### 5.1. Molecular docking simulations

The structures of oleacein (PubChem CID: 18684078) and tolcapone (PubChem CID: 4659569) were obtained from the National Center for Biotechnology Information (NCBI) PubChem database (http://www.ncbi.nlm.nih.gov/pccompound). The atomic coordinates of the COMT protein were obtained from PDB using either the PDB 3BWM (parental COMT) or 3BWY (COMT V108M). COMT structure was subjected to geometry optimization using the repair function of the FoldX algorithm (Schymkowitz et al., 2005). Molecular docking experiments were performed with AutoDock/Vina using YASARA dynamics v18.12.27 software (Krieger and Vriend, 2014; Winkler et al., 2019), as previously described (Encinar et al., 2015; Galiano et al., 2016; Ruiz-Torres et al., 2018). A total of 700 flexible docking runs were set and clustered around the putative binding sites. Two complexed compounds were considered to belong to different clusters of hot spot conformations if the ligand RMSD of their atomic positions was larger than a minimum of 6 Å. The YASARA pH command was set to 7.4. The YASARA software calculated the Gibbs free energy variation (ΔG, kcal/mol), with more positive energy values indicating stronger binding. Values included in Fig. 1 are with a negative sign. All the figures were prepared using the PyMol 2.0 software and all the interactions were detected using the PLIP algorithm (Salentin et al., 2015).

### 5.2. Molecular dynamics simulations

YASARA dynamics v18.12.27 was also used for all the MD simulations with AMBER14 as a force field. The simulation cell was allowed to include 20 Å surrounding the protein and filled with water at a density of 0.997 g/mL. Initial energy minimization was carried out under relaxed constraints using steepest descent minimization. Simulations were performed in water at constant pressure-constant temperature (25 °C) conditions. To mimic physiological conditions, counter ions were added to neutralize the system; $Na^+$ or $Cl^-$ were added in replacement of water to give a total NaCl concentration of 0.9% and pH was maintained at 7.4. Hydrogen atoms were added to the protein structure at the appropriate ionizable groups according to the calculated pKa in relation to the simulation pH (i.e., a hydrogen atom will be added if the computed pKa is higher than the pH). The pKa was computed for each residue according to the Ewald method (Krieger et al., 2006). All simulation steps were run by a preinstalled macro (md_run.mcr) within the YASARA suite. Data were collected every 100 ps.

TMM/PBSA was implemented with the YASARA macro md_analyzebindenergy.mcr to calculate the binding free energy with solvation of the ligand, complex, and free protein for the COMT native and V108M form complexes. The binding free energy (kcal/mol) was expressed according to the following equation:

$$\Delta E_{binding} = [poterec(i) + solverec(i) + potelig + solvelig] - [potecmp(i) + solvecmp(i)]$$

where i is the position number, “pote” is the **pot**ential **e**nergy for the complex (*potecmp*), free protein (*poterec*), or free ligand (*potelig*), and “solve” is the **sol**vation **e**nergy for the complex (*solvecmp*), free protein (*solverec*), or free ligand (*solvelig*). More positive binding free values indicate better binding.

### 5.3. Quantum mechanics/molecular mechanics calculations

Taking advantage of the similarity between the catechol and the oleacein dihydroxy-phenol moiety, oleacein was superimposed over the catechol-binding site of COMT and forced to maintain the interactions with the atomic positions involved in the methyl transfer from the SAM

cofactor. This system was then solvated and equilibrated by means of a short MD simulation. As suggested by the catechol literature, we chose the bidentate coordination of the oleacein molecule to a COMT active site containing the $Mg^{2+}$ ion (Lau and Bruice, 1998; Bonifácio et al., 2007; Law et al., 2016; Patra et al., 2016). The system set-up and all the calculations were performed using the dynamo program (Field, 2008) coupled to ORCA v3.0.3 (Neese, 2012). Graphical representations were prepared using VMD v1.9.1.

### 5.4. Oleacein isolation and purification

Oleacein (decarboxymethyl oleuropein aglycone) was isolated and purified from the phenolic fraction of EVOO as described previously (Corominas-Faja et al., 2018).

### 5.5. COMT activity assays

COMT and V108M COMT activity assays were performed using the Flashplate Catechol O-methyltransferase service (Reaction Biology Corp., Malvern, PA, USA). Oleacein was dissolved in DMSO at a stock concentration of 10 mmol/L and tested in 10-dose $IC_{50}$ mode with a 2-fold serial dilution in duplicate (COMT) or singlet (COMT V108M), starting at 100 μmol/L. Tolcapone was tested in 10-dose $IC_{50}$ mode with a 3-fold serial dilution starting at 1 μmol/L. The reaction (i.e., S-adenosyl-L-[methyl]-$^{3}$H]methionine + catechol → S-adenosyl-L-homocysteine + guaiacol [methyl-$^{3}$H]) was carried out in the presence of 1 μmol/L SAM, whereas the catechol substrate was at 0.5 μmol/L. A no-inhibitor control was considered 100%. Curve fits were performed where the enzymes activities at the highest concentration of compounds were less than 65%.

## Funding

Work in the Menendez laboratory is supported by the Spanish Ministry of Science and Innovation (Grant SAF2016-80639-P, Plan Nacional de I+D+I, founded by the European Regional Development Fund, Spain) and by an unrestricted research grant from the Fundació Oncolliga Girona (Lliga catalana d'ajuda al malalt de càncer, Girona). Work in the Encinar laboratory is supported by Project AGL2015-67995-C3-1-R from the Spanish Ministry of Economy and Competitiveness (MINECO) and PROMETEO/2016/006 grants from Generalitat Valenciana.

## Acknowledgments

We are grateful to the Cluster of Scientific Computing (http://ccc.umh.es/) of the Miguel Hernandez University (UMH) and the Centro de Supercomputación (ALHAMBRA-CSIRC) of the University of Granada for supporting supercomputing facilities. The authors would like to thank Dr. Kenneth McCreath for editorial support.

## Appendix A. Supplementary data

Supplementary data to this article can be found online at https://doi.org/10.1016/j.fct.2019.03.049.

## Transparency document

Transparency document related to this article can be found online at https://doi.org/10.1016/j.fct.2019.03.049.

## References

Angeloni, C., Malaguti, M., Barbalace, M.C., Hrelia, S., 2017. Bioactivity of olive oil phenols in neuroprotection. Int. J. Mol. Sci. 18 pii:E2230.

Antypa, N., Drago, A., Serretti, A., 2013. The role of COMT gene variants in depression: bridging neuropsychological, behavioral and clinical phenotypes. Neurosci. Biobehav. Rev. 37, 1597–1610.

Bai, H.W., Shim, J.Y., Yu, J., Zhu, B.T., 2007. Biochemical and molecular modeling studies of the O-methylation of various endogenous and exogenous catechol substrates catalyzed by recombinant human soluble and membrane-bound catechol-O-methyltransferases. Chem. Res. Toxicol. 20, 1409–1425.

Bendini, A., Cerretani, L., Carrasco-Pancorbo, A., Gómez-Caravaca, M.A., Segura-Carretero, A., Fernández-Gutiérrez, A., Lercker, G., 2007. Phenolic molecules in virgin olive oils: a survey of their sensory properties, health effects, antioxidant activity and analytical methods. An overview of the last decade. Molecules 12, 1679–1719.

Bode, A.M., Dong, Z., 2009. Epigallocatechin 3-gallate and green tea catechins: united they work, divided they fail. Cancer Prev. Res. 2, 514–517.

Bonifácio, M.J., Palma, P.N., Almeida, L., Soares-da-Silva, P., 2007. Catechol-O-methyltransferase and its inhibitors in Parkinson's disease. CNS Drug Rev. 13, 352–379.

Brandt, W., Manke, K., Vogt, T., 2015. A catalytic triad–Lys-Asn-Asp–Is essential for the catalysis of the methyl transfer in plant cation-dependent O-methyltransferases. Phytochemistry 113, 130–139.

Casamenti, F., Stefani, M., 2017. Olive polyphenols: new promising agents to combat aging-associated neurodegeneration. Expert Rev. Neurother. 17, 345–358.

Chen, Y., Yu, X., Li, T., Yan, H., Mo, Z., 2016. Significant association of catechol-O-methyltransferase Val158Met polymorphism with bladder cancer instead of prostate and kidney cancer. Int. J. Biol. Mark. 31, e110–117.

Cheng, X., 1995. Structure and function of DNA methyltransferases. Annu. Rev. Biophys. Biomol. Struct. 24, 293–318.

Colomer, R., Lupu, R., Papadimitropoulou, A., Vellon, L., Vazquez-Martin, A., Brunet, J., Fernandez-Gutierrez, A., Segura-Carretero, A., Menendez, J.A., 2008. Giacomo Castelvetro's salads. Anti-HER2 oncogene nutraceuticals since the 17th century? Clin. Transl. Oncol. 10, 30–34.

Corominas-Faja, B., Cuyas, E., Lozano-Sanchez, J., Cufi, S., Verdura, S., Fernandez-Arroyo, S., Borras-Linares, I., Martin-Castillo, B., Martin, A.G., Lupu, R., et al., 2018. Extra-virgin olive oil contains a metabolo-epigenetic inhibitor of cancer stem cells. Carcinogenesis 39, 601–613.

Corominas-Faja, B., Santangelo, E., Cuyas, E., Micol, V., Joven, J., Ariza, X., Segura-Carretero, A., Garcia, J., Menendez, J.A., 2014. Computer-aided discovery of biological activity spectra for anti-aging and anti-cancer olive oil oleuropeins. Aging (N Y) 6, 731–741.

Crespo, M.C., Tome-Carneiro, J., Davalos, A., Visioli, F., 2018. Pharma-nutritional properties of olive oil phenols. Transfer of new findings to human nutrition. Foods 7 pii:E90.

De la Torre, R., Corella, D., Castaner, O., Martinez-Gonzalez, M.A., Salas-Salvador, J., Vila, J., Estruch, R., Sorli, J.V., Aros, F., Fiol, M., et al., 2017. Protective effect of homovanillyl alcohol on cardiovascular disease and total mortality: virgin olive oil, wine, and catechol-methylathion. Am. J. Clin. Nutr. 105, 1297–1304.

Encinar, J.A., Fernandez-Ballester, G., Galiano-Ibarra, V., Micol, V., 2015. In silico approach for the discovery of new PPARgamma modulators among plant-derived polyphenols. Drug Des. Dev. Ther. 9, 5877–5895.

Fang, M., Chen, D., Yang, C.S., 2007. Dietary polyphenols may affect DNA methylation. J. Nutr. 137, 223S–228S.

Fang, M.Z., Wang, Y., Ai, N., Hou, Z., Sun, Y., Lu, H., Welsh, W., Yang, C.S., 2003. Tea polyphenol (-)-epigallocatechin-3-gallate inhibits DNA methyltransferase and reactivates methylation-silenced genes in cancer cell lines. Cancer Res. 63, 7563–7570.

Field, M.J., 2008. The pDynamo program for molecular simulations using hybrid quantum chemical and molecular mechanical potentials. J. Chem. Theory Comput. 4, 1151–1161.

Forester, S.C., Lambert, J.D., 2014. Synergistic inhibition of lung cancer cell lines by (-)-epigallocatechin-3-gallate in combination with clinically used nitrocatechol inhibitors of catechol-O-methyltransferase. Carcinogenesis 35, 365–372.

Fuccelli, R., Rosignoli, P., Servili, M., Veneziani, G., Taticchi, A., Fabiani, R., 2018. Genotoxicity of heterocyclic amines (HCAs) on freshly isolated human peripheral blood mononuclear cells (PBMC) and prevention by phenolic extracts derived from olive, olive oil and olive leaves. Food Chem. Toxicol. 122, 234–241.

Galiano, V., Garcia-Valtanen, P., Micol, V., Encinar, J.A., 2016. Looking for inhibitors of the dengue virus NS5 RNA-dependent RNA-polymerase using a molecular docking approach. Drug Des. Dev. Ther. 10, 3163–3181.

Garcia-Villalba, R., Carrasco-Pancorbo, A., Oliveras-Ferraros, C., Menendez, J.A., Segura-Carretero, A., Fernandez-Gutierrez, A., 2012. Uptake and metabolism of olive oil polyphenols in human breast cancer cells using nano-liquid chromatography coupled to electrospray ionization-time of flight-mass spectrometry. J. Chromatogr. B Analyt. Technol. Biomed. Life Sci. 898, 69–77.

Genheden, S., Ryde, U., 2015. The MM/PBSA and MM/GBSA methods to estimate ligand-binding affinities. Expert Opin. Drug Discov. 10, 449–461.

Goya, L., Mateos, R., Bravo, L., 2007. Effect of the olive oil phenol hydroxytyrosol on human hepatoma HepG2 cells. Protection against oxidative stress induced by tert-butylhydroperoxide. Eur. J. Nutr. 46, 70–78.

Hall, K.T., Buring, J.E., Mukamal, K.J., Vinayaga Moorthy, M., Wayne, P.M., Kaptchuk, T.J., Battinelli, E.M., Ridker, P.M., Sesso, H.D., Weinstein, S.J., Albanes, D., Cook, N.R., Chasman, D.I., 2019. COMT and alpha-tocopherol effects in cancer prevention: gene-supplement interactions in two randomized clinical trials. J. Natl. Cancer Inst. https://doi.org/10.1093/jnci/djy204. ([Epub ahead of print]).

He, Q., Xue, G., Chen, C., Lu, Z.L., Chen, C., Lei, X., Liu, Y., Li, J., Zhu, B., Moyzis, R.K., et al., 2012. COMT Val158Met polymorphism interacts with stressful life events and parental warmth to influence decision making. Sci. Rep. 2, 677.

Huang, D., Cui, L., Ahmed, S., Zainab, F., Wu, Q., Wang, X., Yuan, Z., 2019. An overview of epigenetic agents and natural nutrition products targeting DNA methyltransferase, histone deacetylases and microRNAs. Food Chem. Toxicol. 123, 574–594.

Huang, E., Zai, C.C., Lisoway, A., Maciukiewicz, M., Felsky, D., Tiwari, A.K., Bishop, J.R., Ikeda, M., Molero, P., Ortuno, F., et al., 2016. Catechol-O-Methyltransferase Val158Met polymorphism and clinical response to antipsychotic treatment in schizophrenia and schizo-affective disorder patients: a meta-analysis. Int. J. Neuropsychopharmacol. 19 pii: pyv132.
Jindal, G., Warshel, A., 2016. Exploring the dependence of QM/MM calculations of enzyme catalysis on the size of the QM region. J. Phys. Chem. B 120, 9913–9921.
Jorga, K., Fotteler, B., Heizmann, P., Gasser, R., 1999. Metabolism and excretion of tolcapone, a novel inhibitor of catechol-O-methyltransferase. Br. J. Clin. Pharmacol. 48, 513–520.
Kamerlin, S.C., Haranczyk, M., Warshel, A., 2009. Progress in ab initio QM/MM free-energy simulations of electrostatic energies in proteins: accelerated QM/MM studies of pKa, redox reactions and solvation free energies. Br. J. Clin. Pharmacol. 113, 1253–1272.
Kang, K.S., Wen, Y., Yamabe, N., Fukui, M., Bishop, S.C., Zhu, B.T., 2010. Dual beneficial effects of (-)-epigallocatechin-3-gallate on levodopa methylation and hippocampal neurodegeneration: in vitro and in vivo studies. PLoS One 5, e11951.
Kiss, L.E., Soares-da-Silva, P., 2014. Medicinal chemistry of catechol O-methyltransferase (COMT) inhibitors and their therapeutic utility. J. Med. Chem. 57, 8692–8717.
Klebe, S., Golmard, J.L., Nalls, M.A., Saad, M., Singleton, A.B., Bras, J.M., Hardy, J., Simon-Sanchez, J., Heutink, P., Kuhlenbaumer, G., et al., 2013. The Val158Met COMT polymorphism is a modifier of the age at onset in Parkinson's disease with a sexual dimorphism. J. Neurol. Neurosurg. Psychiatry 84, 666–673.
Krieger, E., Nielsen, J.E., Spronk, C.A., Vriend, G., 2006. Fast empirical pKa prediction by Ewald summation. J. Mol. Graph. Model. 25, 481–486.
Krieger, E., Vriend, G., 2014. YASARA View - molecular graphics for all devices - from smartphones to workstations. Bioinformatics 30, 2981–2982.
Kulik, H.J., Zhang, J., Klinman, J.P., Martinez, T.J., 2016. How large should the QM region Be in QM/MM calculations? The case of catechol O-methyltransferase. J. Phys. Chem. B 120, 11381–11394.
Lachman, H.M., Papolos, D.F., Saito, T., Yu, Y.M., Szumlanski, C.L., Weinshilboum, R.M., 1996. Human catechol-O-methyltransferase pharmacogenetics: description of a functional polymorphism and its potential application to neuropsychiatric disorders. Pharmacogenetics 6, 243–250.
Land, H., Humble, M.S., 2018. YASARA: a tool to obtain structural guidance in biocatalytic investigations. Methods Mol. Biol. 1685, 43–67.
Landis-Piwowar, K., Chen, D., Chan, T.H., Dou, Q.P., 2010. Inhibition of catechol-Omicron-methyltransferase activity in human breast cancer cells enhances the biological effect of the green tea polyphenol (-)-EGCG. Oncol. Rep. 24, 563–569.
Lau, E.Y., Bruice, T.C., 1998. Importance of correlated motions in forming highly reactive near attack conformations in catechol O methyltransferase. J. Am. Chem. Soc. 120, 12387.
Law, B.J., Bennett, M.R., Thompson, M.L., Levy, C., Shepherd, S.A., Leys, D., Micklefield, J., 2016. Effects of active-site modification and quaternary structure on the regioselectivity of catechol-O-methyltransferase. Angew Chem. Int. Ed. Engl. 55, 2683–2687.
Lee, W.J., Shim, J.Y., Zhu, B.T., 2005. Mechanisms for the inhibition of DNA methyltransferases by tea catechins and bioflavonoids. Mol. Pharmacol. 68, 1018–1030.
Lee, W.J., Zhu, B.T., 2006. Inhibition of DNA methylation by caffeic acid and chlorogenic acid, two common catechol-containing coffee polyphenols. Carcinogenesis 27, 269–277.
Lopez-Miranda, J., Perez-Jimenez, F., Ros, E., De Caterina, R., Badimon, L., Covas, M.I., Escrich, E., Ordovas, J.M., Soriguer, F., Abia, R., et al., 2010. Olive oil and health: summary of the II international conference on olive oil and health consensus report, Jaen and Cordoba (Spain) 2008. Nutr. Metabol. Cardiovasc. Dis. 20, 284–294.
Manna, C., Galletti, P., Maisto, G., Cucciolla, V., D'Angelo, S., Zappia, V., 2000. Transport mechanism and metabolism of olive oil hydroxytyrosol in Caco-2 cells. FEBS Lett. 470, 341–344.
Mannisto, P.T., Kaakkola, S., 1999. Catechol-O-methyltransferase (COMT): biochemistry, molecular biology, pharmacology, and clinical efficacy of the new selective COMT inhibitors. Pharmacol. Rev. 51, 593–628.
Maximova, T., Moffatt, R., Ma, B., Nussinov, R., Shehu, A., 2016. Principles and overview of sampling methods for modeling macromolecular structure and dynamics. PLoS Comput. Biol. 12, e1004619.
McLeod, H.L., Syvanen, A.C., Githang'a, J., Indalo, A., Ismail, D., Dewar, K., Ulmanen, I., Sludden, J., 1998. Ethnic differences in catechol O-methyltransferase pharmacogenetics: frequency of the codon 108/158 low activity allele is lower in Kenyan than Caucasian or South-west Asian individuals. Pharmacogenetics 8, 195–199.
Menendez, J.A., Joven, J., Aragones, G., Barrajon-Catalan, E., Beltran-Debon, R., Borras-Linares, I., Camps, J., Corominas-Faja, B., Cufi, S., Fernandez-Arroyo, S., et al., 2013. Xenohormetic and anti-aging activity of secoiridoid polyphenols present in extra virgin olive oil: a new family of gerosuppressant agents. Cell Cycle 12, 555–578.
Miro-Casas, E., Covas, M.I., Farre, M., Fito, M., Ortuno, J., Weinbrenner, T., Roset, P., de la Torre, R., 2003. Hydroxytyrosol disposition in humans. Clin. Chem. 49, 945–952.
Nagai, M., Conney, A.H., Zhu, B.T., 2004. Strong inhibitory effects of common tea catechins and bioflavonoids on the O-methylation of catechol estrogens catalyzed by human liver cytosolic catechol-O-methyltransferase. Drug Metab. Dispos. 32, 497–504.
Neese, F., 2012. The ORCA program system. Wiley Interdiscip. Rev.: Comput. Mol. Sci. 2, 73–78.
Nikou, T., Liaki, V., Stathopoulos, P., Sklirou, A.D., Tsakiri, E.N., Jakschitz, T., Bonn, G., Trougakos, I.P., Halabalaki, M., Skaltsounis, L.A., 2019. Comparison survey of EVOO polyphenols and exploration of healthy aging-promoting properties of oleocanthal and oleacein. Food Chem. Toxicol. 125, 403–412.
Patra, N., Ioannidis, E.I., Kulik, H.J., 2016. Computational investigation of the interplay of substrate positioning and reactivity in catechol O-methyltransferase. PLoS One 11, e0161868.
Perkovic, M.N., Strac, D.S., Tudor, L., Konjevod, M., Erjavec, G.N., Pivac, N., 2018. Catechol-O-methyltransferase, cognition and alzheimer's disease. Curr. Alzheimer Res. 15, 408–419.
Rigacci, S., 2015. Olive oil phenols as promising multi-targeting agents against alzheimer's disease. Adv. Exp. Med. Biol. 863, 1–20.
Roca, M., Martí, S., Andrés, J., Moliner, V., Tuñón, I., Bertrán, J., Williams, I.H., 2003. Theoretical modeling of enzyme catalytic power: analysis of "cratic" and electrostatic factors in catechol O-methyltransferase. J. Am. Chem. Soc. 125, 7726–7737.
Roston, D., Cui, Q., 2016. QM/MM analysis of transition states and transition state analogues in metalloenzymes. Methods Enzymol. 577, 213–250.
Ruiz-Torres, V., Losada-Echeberria, M., Herranz-Lopez, M., Barrajon-Catalan, E., Galiano, V., Micol, V., Encinar, J.A., 2018. New mammalian target of rapamycin (mTOR) modulators derived from natural product databases and marine extracts by using molecular docking techniques. Mar. Drugs 16 pii:E385.
Rutherford, K., Le Trong, I., Stenkamp, R.E., Parson, W.W., 2008. Crystal structures of human 108V and 108M catechol O-methyltransferase. J. Mol. Biol. 380, 120–130.
Sak, K., 2017. The Val158Met polymorphism in COMT gene and cancer risk: role of endogenous and exogenous catechols. Drug Metab. Rev. 49, 56–83.
Salentin, S., Schreiber, S., Haupt, V.J., Adasme, M.F., Schroeder, M., 2015. PLIP: fully automated protein-ligand interaction profiler. Nucleic Acids Res. 43, W443–447.
Sambataro, F., Pennuto, M., Christian Wolf, R., 2012. Catechol-o-methyl transferase modulates cognition in late life: evidence and implications for cognitive enhancement. CNS Neurol. Disord. - Drug Targets 11, 195–208.
Schymkowitz, J., Borg, J., Stricher, F., Nys, R., Rousseau, F., Serrano, L., 2005. The FoldX web server: an online force field. Nucleic Acids Res. 33, W382–388.
Serreli, G., Melis, M.P., Corona, G., Deiana, M., 2019. Modulation of LPS-induced nitric oxide production in intestinal cells by hydroxytyrosol and tyrosol metabolites: insight into the mechanism of action. Food Chem. Toxicol. 125, 520–527.
Serretti, A., Olgiati, P., 2012. Catechol-o-methyltransferase and Alzheimer's disease: a review of biological and genetic findings. CNS Neurol. Disord. - Drug Targets 11, 299–305.
Servili, M., Esposto, S., Fabiani, R., Urbani, S., Taticchi, A., Mariucci, F., Selvaggini, R., Montedoro, G.F., 2009. Phenolic compounds in olive oil: antioxidant, health and organoleptic activities according to their chemical structure. Inflammopharmacology 17, 76–84.
Shimizu, M., Deguchi, A., Lim, J.T., Moriwaki, H., Kopelovich, L., Weinstein, I.B., 2005. (-)-Epigallocatechin gallate and polyphenon E inhibit growth and activation of the epidermal growth factor receptor and human epidermal growth factor receptor-2 signaling pathways in human colon cancer cells. Clin. Cancer Res. 11, 2735–2746.
Skates, E., Overall, J., DeZego, K., Wilson, M., Esposito, D., Lila, M.A., Komarnytsky, S., 2018. Berries containing anthocyanins with enhanced methylation profiles are more effective at ameliorating high fat diet-induced metabolic damage. Food Chem. Toxicol. 111, 445–453.
Soler, A., Romero, M.P., Macià, A., Saha, S., Furniss, C.S.M., Kroon, P.A., Motilva, M.J., 2010. Digestion stability and evaluation of the metabolism and transport of olive oil phenols in the human small-intestinal epithelial Caco-2/TC7 cell line. Food Chem. 119, 703–714.
Sparta, M., Alexandrova, A.N., 2012. How metal substitution affects the enzymatic activity of catechol-o-methyltransferase. PLoS One 7, e47172.
Suganuma, M., Okabe, S., Kai, Y., Sueoka, N., Sueoka, E., Fujiki, H., 1999. Synergistic effects of (–)-epigallocatechin gallate with (–)-epicatechin, sulindac, or tamoxifen on cancer-preventive activity in the human lung cancer cell line PC-9. Cancer Res. 59, 44–47.
Tomé-Carneiro, J., Crespo, M.C., García-Calvo, E., Luque-García, J.L., Dávalos, A., Visioli, F., 2017. Proteomic evaluation of mouse adipose tissue and liver following hydroxytyrosol supplementation. Food Chem. Toxicol. 107, 329–338.
Trott, O., Olson, A.J., 2010. AutoDock Vina: improving the speed and accuracy of docking with a new scoring function, efficient optimization, and multithreading. J. Comput. Chem. 31, 455–461.
Tsao, D., Liu, S., Dokholyan, N.V., 2011. Regioselectivity of catechol O-methyltransferase confers enhancement of catalytic activity. Chem. Phys. Lett. 506, 135–138.
Vazquez-Martin, A., Fernandez-Arroyo, S., Cufi, S., Oliveras-Ferraros, C., Lozano-Sanchez, J., Vellon, L., Micol, V., Joven, J., Segura-Carretero, A., Menendez, J.A., 2012. Phenolic secoiridoids in extra virgin olive oil impede fibrogenic and oncogenic epithelial-to-mesenchymal transition: extra virgin olive oil as a source of novel antiaging phytochemicals. Rejuvenation Res. 15, 3–21.
Viciano, I., Castillo, R., Martí, S., 2015. QM/MM modeling of the hydroxylation of the androstenedione substrate catalyzed by cytochrome P450 aromatase (CYP19A1). J. Comput. Chem. 36, 1736–1747.
Wang, C., Nguyen, P.H., Pham, K., Huynh, D., Le, T.B., Wang, H., Ren, P., Luo, R., 2016. Calculating protein-ligand binding affinities with MMPBSA: method and error analysis. J. Comput. Chem. 37, 2436–2446.
Wang, P., Heber, D., Henning, S.M., 2012. Quercetin increased bioavailability and decreased methylation of green tea polyphenols in vitro and in vivo. Food Funct. 3, 635–642.
Wang, P., Vadgama, J.V., Said, J.W., Magyar, C.E., Doan, N., Heber, D., Henning, S.M., 2014. Enhanced inhibition of prostate cancer xenograft tumor growth by combining quercetin and green tea. J. Nutr. Biochem. 25, 73–80.
Winkler, S., Derler, R., Gesslbauer, B., Krieger, E., Kungl, A.J., 2019. Molecular dynamics simulations of the chemokine CCL2 in complex with pull down-derived heparan sulfate hexasaccharides. Biochim. Biophys. Acta Gen. Subj. 1863, 528–533.
Witte, A.V., Floel, A., 2012. Effects of COMT polymorphisms on brain function and behavior in health and disease. Brain Res. Bull. 88, 418–428.
Wu, A.H., Arakawa, K., Stanczyk, F.Z., Van Den Berg, D., Koh, W.P., Yu, M.C., 2005. Tea and circulating estrogen levels in postmenopausal Chinese women in Singapore.

Carcinogenesis 26, 976–980.
Wu, A.H., Tseng, C.C., Van Den Berg, D., Yu, M.C., 2003a. Tea intake, COMT genotype, and breast cancer in Asian-American women. Cancer Res. 63, 7526–7529.
Wu, A.H., Yu, M.C., Tseng, C.C., Hankin, J., Pike, M.C., 2003b. Green tea and risk of breast cancer in Asian Americans. Int. J. Cancer 106, 574–579.
Zhou, Q., Wang, Y., Chen, A., Tao, Y., Song, H., Li, W., Tao, J., Zuo, M., 2015. Association between the COMT Val158Met polymorphism and risk of cancer: evidence from 99 case-control studies. OncoTargets Ther. 8, 2791–2803.
Zhu, B.T., 2002. Catechol-O-Methyltransferase (COMT)-mediated methylation metabolism of endogenous bioactive catechols and modulation by endobiotics and xenobiotics: importance in pathophysiology and pathogenesis. Curr. Drug Metabol. 3, 321–349.
Zhu, B.T., Conney, A.H., 1998. Is 2-methoxyestradiol an endogenous estrogen metabolite that inhibits mammary carcinogenesis? Cancer Res. 58, 2269–2277.
Zhu, B.T., Liehr, J.G., 1994. Quercetin increases the severity of estradiol-induced tumorigenesis in hamster kidney. Toxicol. Appl. Pharmacol. 125, 149–158.
Zhu, B.T., Liehr, J.G., 1996. Inhibition of catechol O-methyltransferase-catalyzed O-methylation of 2- and 4-hydroxyestradiol by quercetin. Possible role in estradiol-induced tumorigenesis. J. Biol. Chem. 271, 1357–1363.
Zhu, B.T., Patel, U.K., Cai, M.X., Conney, A.H., 2000. O-Methylation of tea polyphenols catalyzed by human placental cytosolic catechol-O-methyltransferase. Drug Metab. Dispos. 28, 1024–1030.
Zhu, B.T., Patel, U.K., Cai, M.X., Lee, A.J., Conney, A.H., 2001. Rapid conversion of tea catechins to monomethylated products by rat liver cytosolic catechol-O-methyltransferase. Xenobiotica 31, 879–890.
Zhu, B.T., Shim, J.Y., Nagai, M., Bai, H.W., 2008. Molecular modelling study of the mechanism of high-potency inhibition of human catechol-O-methyltransferase by (-)-epigallocatechin-3-O-gallate. Xenobiotica 38, 130–146.
Zhu, B.T., Wang, P., Nagai, M., Wen, Y., Bai, H.W., 2009. Inhibition of human catechol-O-methyltransferase (COMT)-mediated O-methylation of catechol estrogens by major polyphenolic components present in coffee. J. Steroid Biochem. Mol. Biol. 113, 65–74.
Zhu, B.T., Wu, K.Y., Wang, P., Cai, M.X., Conney, A.H., 2010. O-methylation of catechol estrogens by human placental catechol-o-methyltransferase: interindividual differences in sensitivity to heat inactivation and to inhibition by dietary polyphenols. Drug Metab. Dispos. 38, 1892–1899.
Zurcher, G., Da Prada, M., 1982. Rapid and sensitive single-step radiochemical assay for catechol-O-methyltransferase. J. Neurochem. 38, 191–195.